



Title	Organization of spin- and redox-labile metal centers into Langmuir and Langmuir-Blodgett films
Authors(s)	Gandolfi, Claudio, Miyashita, Naoko, Kurth, Dirk G., Martinho, Paulo N., Morgan, Grace G., Albrecht, Martin
Publication date	2010
Publication information	Gandolfi, Claudio, Naoko Miyashita, Dirk G. Kurth, Paulo N. Martinho, Grace G. Morgan, and Martin Albrecht. "Organization of Spin- and Redox-Labile Metal Centers into Langmuir and Langmuir-Blodgett Films." RSC Publishing, 2010. https://doi.org/10.1039/B926023D .
Publisher	RSC Publishing
Item record/more information	http://hdl.handle.net/10197/3737
Publisher's version (DOI)	10.1039/B926023D

Downloaded 2026-05-01 23:35:31

The UCD community has made this article openly available. Please share how this access benefits you. Your story matters! (@ucd_oa)



© Some rights reserved. For more information

Organization of spin- and redox-labile metal centers into Langmuir and Langmuir-Blodgett films

Claudio Gandolfi,^a Naoko Miyashita,^b Dirk G. Kurth,^b Paulo N. Martinho,^c Grace G. Morgan^c and Martin Albrecht^{*a,c}

⁵ Received (in XXX, XXX) Xth XXXXXXXXXX 200X, Accepted Xth XXXXXXXXXX 200X

First published on the web Xth XXXXXXXXXX 200X

DOI: 10.1039/b000000x

New sal₂(trien) ligands that contain alkoxy substituents of various length in meta position of the salicyl entities were coordinated to electronically and magnetically active iron(III) and cobalt(III) centers. The electrochemical and spectroscopic properties of these amphiphilic complexes are virtually unaffected upon alteration of the alkoxy substituents, thus providing a system in which the physical behavior and the metal-centered chemical activity can be tailored independently. The amphiphilic character has been exploited for preparing Langmuir monolayers at the air-water interface and for constructing Langmuir-Blodgett films, hence allowing for hierarchical assembling of electronically and magnetically active systems. While Langmuir films were stable, transfer onto solid supports was limited, which restricted the magnetic analysis of the Langmuir-Blodgett assemblies.

Introduction

Many metal-centered processes are amplified if the active sites are operating in a cooperative fashion.¹ A classic example for such enhanced activity due to cooperation is the spin transition in spin-labile complexes.^{2,3} Synchronized spin crossover typically results in abrupt transitions, often accompanied by a hysteresis, while non-cooperative transitions are gradual and hence much less attractive. Hierarchical self-assembly,⁴ that is, supramolecular organization that is controlled in at least one dimension by stepwise growth, constitutes a useful concept for achieving cooperativity.⁵ In order to effectively allow for tailoring structure and function independently, this concept requires a proper separation of structurally directing elements from active sites such as spin crossover centers.⁶ A major advantage of this concept then consists of the possibility to extrapolate structural trends to other functional entities. For example, layer-by-layer deposition⁷ has become a widely applicable method for the arrangement of functional units of great variety on a surface.⁸

We have applied this concept by using potentially spin- and redox-labile metal complexes of the dianionic sal₂(trien) ligand (Fig. 1), a system that has been well-studied for spin crossover.⁹ Ligand functionalization with a methoxy group at the aryl ring (R = OMe) was reported to affect the spin crossover and the redox activity of the metal center only marginally.^{9c} This position hence offers a suitable anchor for covalently installing entities for supramolecular engineering without affecting the bonding situation around the metal center. Similar to amine functionalization,¹⁰ aryl substitution addresses two mutually *cis*-oriented donor sites of the sal₂(trien) ligand. Introduction of lipophilic substituents therefore provides a methodology for evoking amphiphilic behavior of the molecule, especially when bound to a M^{III}

metal center that induces an ionic coordination environment. Systems with pronounced amphiphilic character tend to self-assemble, for example into Langmuir films at the air-water interface.¹¹ This methodology is often more predictable than crystal engineering¹² for organizing the redox- and spin-crossover active metal centers in a distinct arrangement.¹³ In addition to this two-dimensional self-assembly at the air-water interface, stepwise organization of the material into the third dimension can be achieved through repetitive immobilization of layers onto a support. Such Langmuir-Blodgett (LB) film fabrication ideally affords multilayered systems with a hierarchical structure. While films of spin crossover-active iron(II) complexes have been known, the use of iron(III) complexes for film fabrication is rare.^{13,14} This is surprising when considering the pronounced stability of Fe^{III} towards oxidation at the air-water interface. Moreover, we have recently evidenced the improved activity of such assembled systems in solution.¹⁵ By expanding these efforts, we here report on the synthesis of different redox-active and potentially spin-labile Co^{III} and Fe^{III} complexes comprising variably long alkyl chains in the sal₂(trien) aryl backbone and on the parameters that are relevant for assembling these systems into Langmuir and Langmuir-Blodgett films. Preliminary analysis of mono and bilayer structures suggests that in contrast to solid material, the self-assembled films do undergo spin-crossover.

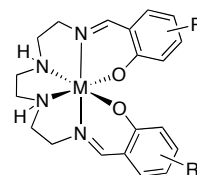
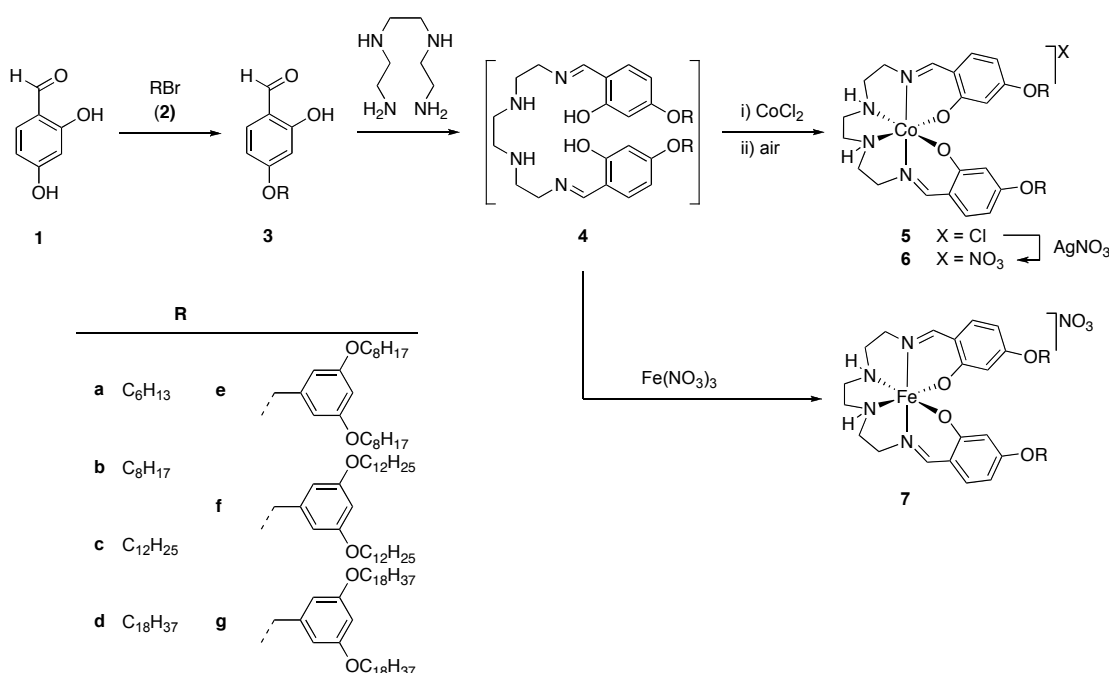


Fig. 1 Sal₂(trien) complexes for remote functionalization via substitution of the phenoxide fragment.



Scheme 1 Synthesis of amphiphilic iron(III) and cobalt(III) complexes.

Results and Discussion

Cobalt(III) and iron(III) complexes

Functionalization of 4-hydroxy salicylaldehyde **1** according to published methods¹⁶ facilitated the introduction of alkyl chains of variable length in the phenolic part of the ligand precursor, thus affording the aldehydes **3a–d** (Scheme 1). The regioselectivity of alkylation was confirmed by nOe effects between the α -protons of the alkyl chain and the two aryl protons *meta* to the aldehyde. In a similar manner, two lipophilic side chains per phenolic unit were incorporated by using the benzylbromides **2e–g** containing two alkoxy-residues in the 3,5-positions,¹⁷ thus yielding the bulkier aldehydes **3e–g** in good yields, even when performing the reaction on a multigram scale.

Subsequent condensation with triethylenetetramine (trien) gave the potentially hexadentate ligand precursors **4**, which were metallated either after isolation or preferably *in situ* due to the sensitivity of **4** towards hydrolysis.¹⁸ Reaction with CoCl₂ and subsequent standing in air gave the corresponding cobalt(III) complexes **5**. Acceleration of metal oxidation by saturating the reaction mixture with O₂ lowered the yields of **5** substantially, suggesting that initial metal coordination requires a cobalt(II) center. The non-coordinating counter anion in **5** was readily displacable because of the high solubility of **5** in organic solvents. Thus, stirring a solution of **5** in THF in the presence of AgNO₃ gave the corresponding nitrate salts **6** in excellent yields. The new iron(III) complexes **7e–g** were synthesized analogously to the previously reported alkyl functionalized complexes **7a–d**.¹⁵

While the paramagnetic nature of the iron complexes **7** precluded NMR investigations, the corresponding cobalt complexes were diamagnetic. The NMR spectra of complexes

5 consistently indicate a symmetrical arrangement of ligand, as only half of the expected number of signals is apparent. All methylene protons are diastereotopic, thus pointing to a rigid chelation of the hexadentate ligand. While different isomers were proposed for unfunctionalized complexes,^{18b} our results suggest that long alkyl chains restrict fluxional processes. A symmetrical arrangement is consistent with the *trans* imine configuration as shown in Scheme 1 (*cf* crystallographic analyses below). Complexation is indicated by small but diagnostic low-field shifts of the aromatic and the imine protons ($\Delta\delta$ 0.1) in the pertinent ¹H NMR spectra. The largest displacements were noted for the CH₂ protons attached to the imine donor site, which shift approximately 0.5 ppm downfield upon cobalt coordination.

Structural analyses of the iron(III) complexes **7** is more limited. Single crystals of **7a** were obtained, though the refinement did not converge due to strong disorder and weak diffraction. Nevertheless, a connectivity pattern around the iron center was established that was in agreement with the arrangement deduced from solution NMR-analysis of the cobalt complexes **5**. Together with the crystal structure previously determined for **7b**,¹⁵ these results suggest that the complexes generally adopt a conformation as shown in Scheme 1, including a mutual *cis* arrangement of both the phenolate units and the amine donors, and a *trans* orientation of the imine ligands.

All complexes were analyzed by electrochemistry. The cobalt(III) complexes undergo an irreversible reduction at around -0.8 V, irrespective of the nature of the counter anion.¹⁹ In contrast, cyclic voltammetry on the iron(III) complexes **7** revealed a reversible reduction of the metal center at -0.55 V (*vs.* SCE; Table 1).²⁰ The reduction potentials for all iron(III) complexes are essentially identical and indicate that functionalization of the phenolate unit does

Table 1 Electrochemical and spectroscopic data of Iron(III) complexes

complex	R	$E_{1/2}$ (V)	ΔE (mV)	λ_{\max} (nm)	ϵ ($M^{-1}cm^{-1}$)	$\nu_{C=N}$
	H	-0.45	134	497	3290	1622
7a	C_6H_{13}	-0.51	176	497	4350	1604
7b	C_8H_{17}	-0.50	161	497	4610	1604
7c	$C_{12}H_{25}$	-0.45	121	497	4760	1604
7d	$C_{18}H_{37}$	-0.50	131	497	4070	1604
7e	$C_6H_3-(C_8H_{17})_2$	-0.51	255	496	4180	1602
7f	$C_6H_3-(C_{12}H_{25})_2$	-0.48	338	497	3460	1603
7g	$C_6H_3-(C_{18}H_{37})_2$	-0.53	224	494	3900	1602

^a All measurements in CH_2Cl_2 solution; $E_{1/2}$ vs SCE, Pt working electrode, scan rate 100 mV s^{-1} and $0.1\text{ M } nBu_4PF_6$ as supporting electrolyte. Fc^+/Fc as internal standard ($E_{1/2} = +0.46\text{ V}$).

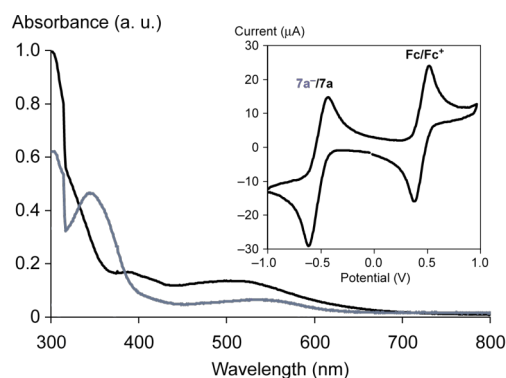


Fig. 2 Spectrophotometric comparison of **7a** (black) and $[7a]^-$ (grey), generated electrochemically by applying a potential of -0.55 V . The inset shows the cyclic voltammogram of **7a**.

not alter the electronic properties of the metal center. Obviously, the electronic activity of the metal center is not affected by variation of the structurally directing hydrophobic tails. Further support for an effective separation of structural and functional elements in complexes **7** was obtained from spectroscopic analyses using UV-vis and IR techniques. Modification of the alkyl tail length (**7a–d**) or the number of alkyl chains (**7e–g**) had virtually no impact on the low-energy absorption wave-length in the visible region (λ_{\max}), attributed to a ligand-to-metal charge transfer. This band is expected to be highly sensitive to modifications in the ligand donor properties and to changes in the ligand coordination geometry.

Spectroelectrochemical measurements using an optically transparent thin layer electrode (OTTLE) cell²¹ allowed the electrochemically generated iron(II) complexes to be characterized *in situ*. For example in complex **7a**, a bathochromic shift of the absorption maximum to 536 nm was noted upon reduction. In addition a new maximum at 346 nm is observed, perhaps due to a ligand centered process.²²

20 Self-assembly

The potential of the functionalized complexes to form organized structures was probed at the air-water interface and on highly ordered pyrolytic graphite (HOPG). Representative AFM imaging (Fig. 3) indicate that simple spin coating induces only little organization of complex **7d**. Upon annealing at $90\text{ }^\circ\text{C}$, however, nanosize domains form that reflect the affinity of the complexes to aggregate and self-assemble.

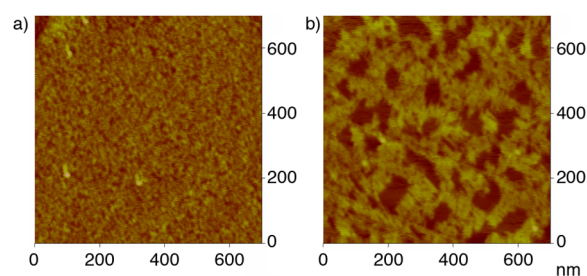


Fig. 3 Complex **7d** spin-coated on highly ordered pyrolytic graphite (HOPG), (a) before and (b) after annealing ($90\text{ }^\circ\text{C}$).

Langmuir films

Langmuir films at the air-water interface were investigated for all complexes **7** and for selected cobalt complexes. Representative pressure-area isotherms and stability plots of the films are shown in Figure 4. These measurements allow for a number of conclusions. First, it appears that a critical number of apolar sites is required in order to achieve high-density films. Complex **7a** does not form films, perhaps due to partial water solubility, while **7b** with short C_8 alkyl chain functionalities does not pack well, which is reflected by the low accessible surface pressure and the steady decrease of the pressure upon keeping the surface constant (Fig. 4a, 4b). This low tendency of film formation may be a consequence of the limited number of apolar molecular recognition sites, inducing only small attractive forces. In addition, the hydrophobic-hydrophilic bias within the molecule may be too small to induce a high tensor difference and hence a preferred orientation of the molecules at the air-water interface. In contrast, films of complexes **7c** and **7d** were stable over extended periods of time ($> 90\text{ min}$) and formed a dense two-dimensional network. Film formation with these complexes was fully reversible and expansion upon pressure release occurred with virtually no hysteresis even after repetitive compression-expansion cycles. The suitability of these complexes for Langmuir films was further supported by monitoring the film forming process by Brewster angle microscopy (BAM),¹⁹ which revealed a homogeneous process without the appearance of specific domains.

When using complexes with twice the number of alkyl chains per head group, *viz.* complexes **7e–g** (Fig. 4c), assembly started earlier, perhaps induced by the larger fractional volume of apolar groups when compared to **7b–d**. The isotherm of films from **7g** provides a rare case where a

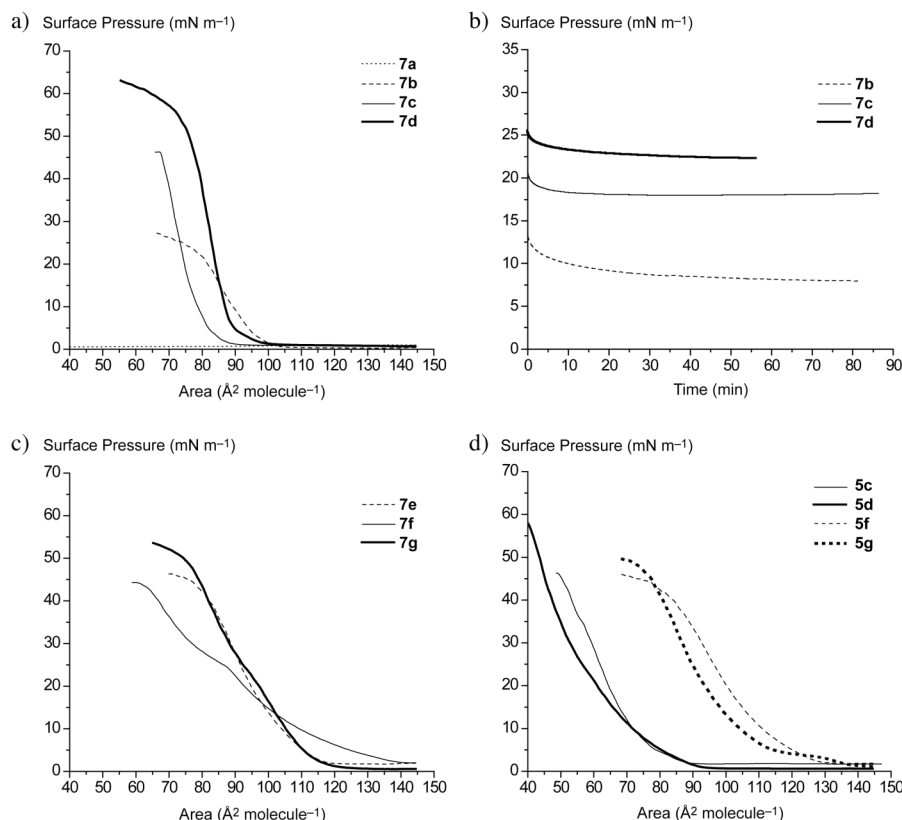


Fig. 4 (a) Pressure-area isotherms for **7a-d** comprising two alkyl chains per iron $\text{sal}_2(\text{trien})$ unit; (b) stability plots at constant surface area for **7b-d**; (c) pressure-area isotherms for **7e-g** comprising four alkyl chains per iron $\text{sal}_2(\text{trien})$ unit; (d) pressure-area isotherms for the cobalt complexes **5c-g**.

distinct transition from the liquid condensed to the solid phase is apparent.²³ No significant differences in terms of stability were observed upon doubling the number of alkyl chains. Irrespective of the number of alkyl chains, the specific molecular area is consistently around 80-85 Å² per molecule, which may seemingly be dictated by the polar iron $\text{sal}_2(\text{trien})$ head group rather than the alkyl tails. However, models based on crystal structure analyses suggest a surface area of the polar iron $\text{sal}_2(\text{trien})$ unit of ca. 65 Å²,⁹ thus requiring three alkyl chains of 20 Å² each for reaching similar projection planes of the polar and apolar fragments.²⁴ Possibly, back folding²⁵ of the alkyl chains in the complexes **7c** and **7d** may occur, thus accounting for the observed surface per molecule ($\sim 4 \times 20$ Å²) and providing an explanation for the similar surface area of the dialkylated complexes with the tetraalkylated (and presumably not back folding) species **7e-g**. Such a model is also consistent with the low film stability of complex **7b**, as back folding is inefficient and less probable with shorter C₈ alkyl chains. Upon increasing the number of C₈ chains to four as in **7e**, back folding is not required any more and the complexes pack densely.

The general features deduced for films comprised of iron(III) complexes are also valid for assembling the analogous cobalt(III) complexes at the air-water interface. High surface pressures up to 60 mN m⁻¹ were accessible with these components. The anion exerted only little influence and films comprising either chloride (**5**) or nitrate (**6**) showed only small differences.¹⁹ Characteristically, however, the surface

area per molecule is markedly influenced by the number of alkyl chains. Films of complexes comprising four alkyl chains (**5f**, **5g**) can be compressed to a minimum area of approximately 80 Å² per molecule (Fig. 4d), which corroborates the results obtained with iron complexes. However when using complexes **5c** or **5d**, functionalized with two alkyl chains only, the minimum area shrinks to ca. 55 Å² per molecule, a value only slightly smaller than the calculated surface of the metal $\text{sal}_2(\text{trien})$ unit. Hence, these results are consistent with a model in which the polar group is limiting the specific surface area if two alkyl groups are used, whereas with complexes containing four alkyl groups, the apolar fraction determines the specific molecular area. While our results do not allow for deduction of a rationale for this distinctly different behavior of iron(III) and cobalt(III) complexes, it is interesting to note that the driving forces for assembly can be swapped by changing the central metal atom. Irrespectively, both types of complexes display a low tendency for hydrolysis in contact with water, as illustrated with the prolonged stability of the Langmuir films.

Transfer of Langmuir films onto supports

Multilayers rather than monolayers, which intrinsically display low signal-to-noise ratios, are often desirable for the fabrication of devices that are potentially useful for electronic or magnetic applications. Multilayer deposition on a solid support and the formation of Langmuir-Blodgett films provides a versatile tool to achieve a hierarchical arrangement of the active units with controlled intermolecular interactions.

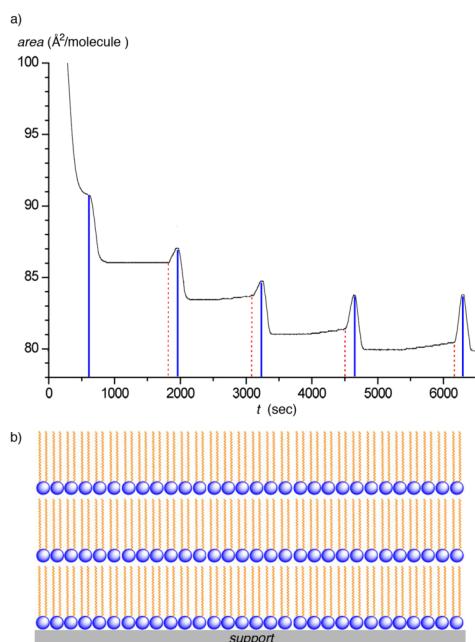


Fig. 5 (a) Langmuir film transfer of **7d** onto glass at 4 mN m^{-1} ; emersion starts are indicated by a solid line, immersions with a dashed line (10-15 min drying after each emersion). (b) Schematic representation of the Z-type LB film deduced from the transfer ratios, blue circles represent the polar head groups and orange lines the alkyl tails.

Table 2 Multilayer deposition of **7d** onto a glass support ^a

layer number	transferred area ($\text{\AA}^2/\text{molecule}$)	transfer ratio
1	4.8	0.87
2	-1.0	-0.18
3	3.6	0.65
4	-1.4	-0.25
5	3.8	0.69
6	-2.9	-0.53
7	3.9	0.74
8	-3.9	-0.74
9	3.9	0.74

^a glass area approximately 7 cm^2 , transfer at $P = 4 \text{ mN m}^{-1}$, at least 10 minutes drying allowed before immersion (even layer numbers).

To this end, the transfer of the iron-containing films from **7d** onto glass was investigated in detail. The transfer ratio was generally high (~ 0.9), though only upon emersion of the support (Table 2, Fig. 5a). During down-stroke the transfer ratios were initially close to zero, indicating that immersion did not result in film transfer. Multilayer fabrication was limited to a maximum of four layers, as subsequent layer deposition occurred only partially (transfer ratio ~ 0.7) and, most significantly, these layers were released again upon immersion. Attempts to increase the number of layers by changing the solid support from glass to silicon wafers or to gold showed no improvement. Modification of the surface pressure during film transfer from 4 to 8 mN/m enhanced the initial transfer ratio (0.97 for first emersion, 0.89 for second emersion), however, only oligolayers were obtained again. Based on the absence of film transfer upon immersion, formation of a Z-type layer may be surmised (Fig. 5b),²⁶ with the polar headgroups oriented towards the support. While we do not have any model so far that may rationalize this unusual

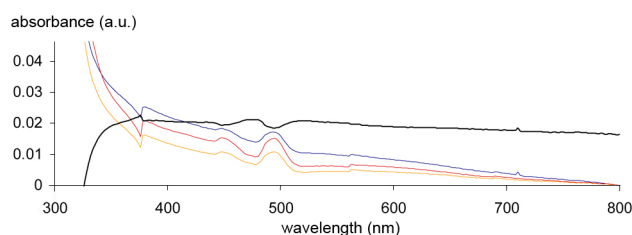


Fig. 6 UV-vis spectroscopic characterization of Langmuir-Blodgett films at 297 K (red), 170 K (orange) and 91 K (blue); difference spectrum of measurements at 297 K and 91 K (black).

Z-type layering,²⁷ clearly, potential applications are attractive due to the anisotropy generated by such a hierarchical organization.

Due to the low transfer ratio, analysis of the physical properties of the film were hampered and spin crossover behavior could not be reliably established. The UV-vis spectrum of the film at 297 K revealed the characteristic high spin absorption around 500 nm (Fig. 6), which is considerably sharper than in solution measurements. Cooling the film to lower temperatures does, however, not indicate a clear transition, as the diagnostic low spin absorption bands around 380 nm and 650 nm are barely detectable. Better film properties and in particular improved transfer ratios may be required, perhaps upon modification of the molecular recognition sites. Work along these lines is currently in progress.

Conclusions

An approach has been developed that allows for functionalization of electronically and magnetically active iron(III) and cobalt(III) complexes with molecular recognition sites at remote positions that do not affect the function of the metal. As a consequence, independent optimization of the structurally directing elements for self-assembly and in parallel of the functional activity is possible in these entities. Using this methodology, stable films were successfully prepared, thus entailing the controlled assembly of potentially redox and spin labile systems. When transferred on a suitable support, such hierarchical assemblies may provide access to magnetically switchable devices with improved metal-metal cooperativity, potentially applicable for example in data storage technology. Independent of the spin transition properties, the redox activity of the film components may constitute an attractive feature for molecular electronics.

Experimental Section

General Comments

The synthesis of the bromides **2e-g**,²⁸ the 4-alkoxy-functionalized salicylaldehydes **3a-d**,²⁹ the aldehydes **3e-g**,¹⁹ and the complexes **7a**, **7b**, and **7d** were reported elsewhere.¹⁵ THF was dried by passage through a solvent purification column. All other reagents were commercially available and were used as received. Flash chromatography was performed using silica gel 60 (63-200 mesh) or basic alox (0.05–0.15 mm, pH 9.5). All ^1H and $^{13}\text{C}\{^1\text{H}\}$ NMR spectra were recorded

at 25 °C on Bruker or Varian spectrometers and referenced to residual solvent ¹H or ¹³C resonances (δ in ppm, *J* in Hz). Assignments are based either on distortionless enhancement of polarization transfer (DEPT) experiments or on homo- and heteronuclear shift correlation spectroscopy. Melting points were determined using an OptiMelt apparatus (Stanford Research Systems) or a Mettler Toledo TGA/SDTA 851 analyzer and are uncorrected. UV-vis measurements were performed on a Perkin Elmer Lambda 40 instrument in CH₂Cl₂ solution (0.2 mM). IR spectra were recorded on a Mattson 5000 FTIR instrument in CHCl₃ solution. High resolution mass spectra and mass spectra were measured by electrospray ionization (ESI-MS) in CHCl₃/MeOH on a Bruker 4.7 T BioAPEX II and a Bruker Daltonics esquire HCT instruments, respectively. Elemental analyses were performed by the Microanalytical Laboratory of Ilse Beetz (Kronach, Germany) and at the ETH Zurich (Switzerland). Electrochemical studies were carried out using an EG&G Princeton Applied Research Potentiostat Model 273A employing a gastight three-electrode cell under an argon atmosphere. A saturated calomel electrode (SCE) was used as reference; a Pt disk (3.14 mm²) and a Pt wire were used as the working and counter electrode, respectively. The redox potentials were measured in dry CH₂Cl₂ (~1 mM) with *n*-Bu₄NPF₆ (0.1 M) as electrolyte and ferrocene (*E*_{1/2} = 0.46 V vs. SCE)³⁰ as internal standard. Spectroelectrochemical studies were carried out in the same electrolytic solution as in the case of cyclic voltammetry using a SPECAC Otlle cell with CaF₂ windows, platinum mesh working, counter electrode and a silver wire reference electrode. The corresponding UV-vis spectra were recorded on a Perkin Elmer Lambda 900 instrument in transmission mode.

Syntheses

Synthesis of 5c. A solution of CoCl₂ × 6H₂O (125 mg, 0.52 mmol) in EtOH (10 mL) was added dropwise to **4c** (378 mg, 0.52 mmol) in warm THF (18 mL) under an Ar atmosphere. The mixture became immediately brown, and was stirred at RT for 20 min and exposed to air for 7 h. The suspension was filtered over a bed of silica and eluted with EtOH/THF 2:1 (80 mL). After evaporation the residue was purified on a short pad of Al₂O₃ by first washing with CHCl₃ (60 mL) and subsequent eluting with EtOH/THF 2:1 (80 mL). After evaporation of the EtOH/THF fraction, the product was redissolved in CHCl₃ (5 mL) and centrifuged. The supernatant was evaporated and dried under reduced pressure to give **5c** as a brown waxy solid (0.43 g, quant.). M.p. 217 °C (decomp.). IR (CHCl₃): 1632 (C=N), 1606 cm⁻¹ (C=C). UV-vis (CH₂Cl₂): λ_{max} (ε) = 377 nm (7460 M⁻¹cm⁻¹). ¹H NMR (CDCl₃, 360 MHz): δ 7.95 (s, 2H, N=CH), 7.03 (d, 2H, *J* = 8.5 Hz, C⁶H), 6.14 (s, 2H, C³H), 6.01 (d, 2H, *J* = 8.1 Hz, C⁵H), 5.04 (s br, 2H, NH), 4.37–4.21 (m, 2H, CH₂N=), 4.09–3.96 (m, 2H, CH₂N=), 3.75–3.62 (m, 4H, CH₂O), 3.17–2.95 (m, 4H, CH₂CH₂N= and NCH₂CH₂N), 2.55–2.41 (m, 2H, NCH₂CH₂N), 2.41–2.23 (m, 2H, CH₂CH₂N=), 1.63–1.48 (m, 4H, CH₂CH₂O), 1.37–1.01 (m, 36H, all CH₂), 0.86 (t, 6H, *J* = 6.6 Hz, CH₃). ¹³C NMR (CDCl₃, 90 MHz): δ 166.7, 164.7 (COBn and COCo), 165.6 (N=CH), 135.5 (C⁶H), 113.2 (CCHN), 105.7 (C⁵H), 104.9

(C³H), 67.9 (OCH₂), 58.6 (CH₂N=), 54.2 (CH₂CH₂N=), 51.9 (NCH₂CH₂N), 32.0, 30.0–29.1, 22.8 (all CH₂), 29.5 (CH₂CH₂O), 26.1 (CH₂CH₂CH₂O), 14.3 (CH₃). MS (ESI): *m/z* = 779.5 [M – Cl]⁺. Anal. found (calcd) for C₄₄H₇₂N₄O₄ClCo (815.47) × 0.5 CHCl₃: C 60.91 (61.07); H 8.68 (8.35); N 5.98 (6.40).

Synthesis of 5d. According to the preparation **5c**, starting from CoCl₂ × 6H₂O (286 mg, 1.2 mmol) in EtOH (12 mL) and **4d** (1.07 g, 1.2 mmol) in THF (42 mL), the title compound was obtained as a brown waxy solid (0.88 g, 78%). M.p. 245 °C (decomp.). IR (CHCl₃): 1634 (C=N), 1606 cm⁻¹ (C=C). UV-vis (CH₂Cl₂): λ_{max} (ε) = 377 nm (7460 M⁻¹cm⁻¹). ¹H NMR (CDCl₃, 360 MHz): δ 7.93 (s, 2H, N=CH), 7.05 (d, 2H, *J* = 8.7 Hz, C⁶H), 6.20 (s, 2H, C³H), 6.08 (d, 2H, *J* = 8.5 Hz, C⁵H), 5.24 (s br, 2H, NH), 4.38–4.18 (m, 2H, CH₂N=), 4.10–3.95 (m, 2H, CH₂N=), 3.74 (t, 4H, *J* = 6.1 Hz, CH₂O), 3.20–2.96 (m, 4H, CH₂CH₂N= and NCH₂CH₂N), 2.48–2.31 (m, 2H, NCH₂CH₂N), 2.31–2.16 (m, 2H, CH₂CH₂N=), 1.70–1.57 (m, 4H, CH₂CH₂O), 1.37–1.01 (m, 60H, all CH₂), 0.86 (t, 6H, *J* = 6.6 Hz, CH₃). ¹³C NMR (CDCl₃, 50 MHz): δ 166.8, 164.8 (COBn and COCo), 165.7 (N=CH), 135.6 (C⁶H), 113.2 (CCHN), 105.9 (C⁵H), 104.9 (C³H), 68.0 (OCH₂), 58.5 (CH₂N=), 54.0 (CH₂CH₂N=), 51.8 (NCH₂CH₂N), 32.0, 29.8–29.2, 22.8 (all CH₂), 26.1 (CH₂CH₂CH₂O), 14.2 (CH₃). MS (ESI): *m/z* = 747.7 [M – Cl]⁺. Anal. found (calcd) for C₅₆H₉₆ClCoN₄O₄ (983.79) × 0.5 CHCl₃: C 64.91 (65.03); H 9.49 (9.32); N 5.28 (5.37); Co 5.53 (5.65).

Synthesis of 5f. Triethylenetetramine (70 mg, 0.48 mmol) was dissolved in EtOH (6 mL) and treated with a solution of **3f** (573 mg, 0.96 mmol) in THF (6 mL). After 15 min stirring at RT, a solution of CoCl₂ × 6H₂O (114 mg, 0.48 mmol) in EtOH (4 mL) was added dropwise under an Ar atmosphere. The mixture became immediately brown and was stirred at RT for 20 min and exposed to air for 7 h. The suspension was filtered over a bed of silica, eluted with EtOH/THF 2:1 (40 mL). After evaporation the residue was purified on a short pad of Al₂O₃ by first washing with CHCl₃ (30 mL) and subsequent eluting with EtOH/THF 2:1 (50 mL). After evaporation of the EtOH/THF fraction the residue was redissolved in pentane (15 mL), filtered through celite and evaporated *in vacuo* to give **5f** as a brown waxy solid (287 mg, 43%). Analytically pure complex aggregated from a solution in Et₂O/MeOH 5:1 by slow evaporation of Et₂O within some days. M.p. 218 °C (decomp.). IR (CHCl₃): 1635 (C=N), 1604 cm⁻¹ (C=C). UV-vis (CH₂Cl₂): λ_{max} (ε) = 377 nm (8130 M⁻¹cm⁻¹). ¹H NMR (CDCl₃, 500 MHz): δ 8.03 (s, 2H, N=CH), 7.14 (d, 2H, *J* = 8.8 Hz, C⁶H), 6.46 (d, 4H, *J* = 2.2 Hz, C⁸H), 6.38–6.35 (m, 4H, C³H and C¹⁰H), 6.23 (dd, 2H, *J* = 8.7, 2.3 Hz, C⁵H), 5.10 (s br, 2H, NH), 4.82 (s, 2H, C^{ar}CH₂O), 4.45–4.33 (m, 2H, CH₂N=), 4.21–4.10 (m, 2H, CH₂N=), 3.88 (t, 4H, *J* = 6.6 Hz, CH₂O), 3.32–3.13 (m, 4H, CH₂CH₂N= and NCH₂CH₂N), 2.57–2.47 (m, 2H, NCH₂CH₂N), 2.45–2.35 (m, 2H, CH₂CH₂N=), 1.79–1.67 (m, 4H, CH₂CH₂O), 1.45–1.19 (m, 72H, all CH₂), 0.87 (t, 6H, *J* = 7.0 Hz, CH₃). ¹³C NMR (CDCl₃, 125 MHz): δ 166.7, 164.7 (COBn and COCo), 165.7 (N=CH), 160.6 (C⁹), 138.8 (C⁷), 135.7 (C⁶H), 113.5 (CCHN), 106.4 (C⁵H), 105.9 (C⁸H), 105.5 (C³H), 100.9 (C¹⁰H), 69.9 (OCH₂C^{ar}), 68.2 (OCH₂), 58.5 (CH₂N=), 53.9 (CH₂CH₂N=),

51.7 (NCH₂CH₂N), 32.1, 30.0–29.2, 22.8 (all CH₂), 26.2 (CH₂CH₂CH₂O), 14.3 (CH₃). MS (ESI): $m/z = 1359.9$ [M – Cl]⁺. Anal. found (calcd) for C₈₂H₁₃₂N₄O₈ClCo (1396.36) × MeOH: C 69.65 (69.79); H 9.40 (9.60); N 3.70 (3.92).

Synthesis of 5g. According to the preparation **5f**, starting from triethylenetetramine (51 mg, 0.35 mmol) in EtOH (2 mL), **3g** (536 mg, 0.70 mmol) in THF (25 mL) and CoCl₂ × 6H₂O (83 mg, 0.35 mmol) in EtOH (3 mL) gave a brown waxy solid (230 mg, 38%). Analytically pure complex was obtained by precipitation with MeOH (30 mL) from an Et₂O (6 mL) solution, followed by precipitation with acetone (30 mL) from pentane (4 mL). M.p. 229 °C (decomp.). IR (CHCl₃): 1635 (C=N), 1603 cm⁻¹ (C=C). UV-vis (CH₂Cl₂): λ_{max} (ε) = 497 nm (8380 M⁻¹cm⁻¹). ¹H NMR (CDCl₃, 360 MHz): δ 7.97 (s, 2H, N=CH), 7.09 (d, 2H, *J* = 8.6 Hz, C⁶H), 6.43 (s br, 4H, C⁸H), 6.38–6.29 (m, 4H, C³H and C¹⁰H), 6.18 (d, 2H, *J* = 8.5 Hz, C⁵H), 5.14 (s br, 2H, NH), 4.75 (s, 2H, C^{ar}CH₂O), 4.40–4.22 (m, 2H, CH₂N=), 4.15–3.98 (m, 2H, CH₂N=), 3.84 (t, 4H, *J* = 6.3 Hz, CH₂O), 3.24–2.98 (m, 4H, CH₂CH₂N= and NCH₂CH₂N), 2.55–2.19 (m, 4H, NCH₂CH₂N and CH₂CH₂N=), 1.76–1.74 (m, 4H, CH₂CH₂O), 1.45–1.09 (m, 120H, all CH₂), 0.87 (t, 6H, *J* = 6.7 Hz, CH₃). ¹³C NMR (CDCl₃, 90 MHz): δ 166.7, 164.4 (COBn and COCo), 165.8 (N=CH), 160.5 (C⁹), 138.7 (C⁷), 135.8 (C⁶H), 113.5 (CCHN), 106.5 (C⁵H), 105.9 (C⁸H), 105.4 (C³H), 100.8 (C¹⁰H), 69.8 (OCH₂C^{ar}), 68.2 (OCH₂), 58.8 (CH₂N=), 54.1 (CH₂CH₂N=), 52.0 (NCH₂CH₂N), 32.1, 30.0–29.2, 22.8 (all CH₂), 26.2 (CH₂CH₂CH₂O), 14.3 (CH₃). MS (ESI): $m/z = 1696.9$ [M – Cl]⁺. Anal. found (calcd) for C₁₀₆H₁₈₀N₄O₈ClCo (1733.01) × 3 MeOH: C 71.48 (71.57); H 10.55 (10.58); N 3.24 (3.06).

General procedure for the synthesis of 6. Chloride complex **5** (0.37 mmol) was dissolved in THF (10 mL) and treated with AgNO₃ (0.37 mol) dissolved in H₂O (5 mL). The mixture was stirred for 2 h in the dark. The mixture was centrifugated and the supernatant evaporated to dryness. The residue was redissolved in CHCl₃ (30 mL) and centrifuged. The supernatant was filtered over Celite, evaporated and dried *in vacuo*.

Complex 6c. Yield: 302 mg (97%). M.p. 232 °C (decomp.). IR (CHCl₃): 1634 (C=N), 1606 cm⁻¹ (C=C). UV-vis (CH₂Cl₂): λ_{max} (ε) = 377 nm (8230 M⁻¹cm⁻¹). ¹H NMR (CDCl₃, 360 MHz): δ 7.98 (s, 2H, N=CH), 7.08 (d, 2H, *J* = 8.4 Hz, C⁶H), 6.25 (s, 2H, C³H), 6.11 (d, 2H, *J* = 8.1 Hz, C⁵H), 4.89 (s br, 2H, NH), 4.33–4.03 (m, 4H, CH₂N=), 3.84–3.70 (m, 4H, CH₂O), 3.23–3.00 (m, 4H, CH₂CH₂N= and NCH₂CH₂N), 2.53–2.26 (m, 4H, NCH₂CH₂N and CH₂CH₂N=), 1.73–1.59 (m, 4H, CH₂CH₂O), 1.44–1.10 (m, 36H, all CH₂), 0.87 (t, 6H, *J* = 6.6 Hz, CH₃).

Complex 6d. Yield: 336 mg (92%). M.p. 239 °C (decomp.). IR (CHCl₃): 1634 (C=N), 1606 cm⁻¹ (C=C). UV-vis (CH₂Cl₂): λ_{max} (ε) = 377 nm (8000 M⁻¹cm⁻¹). ¹H NMR (CDCl₃, 360 MHz): δ 7.99 (s, 2H, N=CH), 7.09 (d, 2H, *J* = 8.7 Hz, C⁶H), 6.26 (s, 2H, C³H), 6.13 (d, 2H, *J* = 8.5 Hz, C⁵H), 4.93 (s br, 2H, NH), 4.36–4.07 (m, 4H, CH₂N=), 3.79 (t, 4H, *J* = 6.3 Hz, CH₂O), 3.26–3.05 (m, 4H, CH₂CH₂N= and NCH₂CH₂N), 2.55–2.30 (m, 4H, CH₂CH₂N= and NCH₂CH₂N), 1.73–1.59 (m, 4H, CH₂CH₂O), 1.41–1.00 (m, 60H, all CH₂), 0.87 (t, 6H, *J* = 6.6 Hz, CH₃).

Complex 6f. Yield: 89 mg (98%). M.p. 187 °C (decomp.). IR

(CHCl₃): 1634 (C=N), 1606 cm⁻¹ (C=C). UV-vis (CH₂Cl₂): λ_{max} (ε) = 377 nm (7990 M⁻¹cm⁻¹). ¹H NMR (CDCl₃, 360 MHz): δ 7.94 (s, 2H, N=CH), 7.07 (d, 2H, *J* = 7.67 Hz, C⁶H), 6.43 (s, 4H, C⁸H), 6.39–6.27 (m, 4H, C³H and C¹⁰H), 6.23 (d, 2H, *J* = 7.9 Hz, C⁵H), 5.02 (s br, 2H, NH), 4.74 (s, 2H, C^{ar}CH₂O), 4.30–4.14 (m, 2H, CH₂N=), 4.14–4.00 (m, 2H, CH₂N=), 3.96–3.76 (m, 4H, CH₂O), 3.18–2.96 (m, 4H, CH₂CH₂N= and NCH₂CH₂N), 2.50–2.21 (m, 4H, CH₂CH₂N= and NCH₂CH₂N), 1.83–1.57 (m, 4H, CH₂CH₂O), 1.51–0.98 (m, 72H, all CH₂), 0.87 (t, 6H, *J* = 6.4 Hz, CH₃).

Synthesis of 7c. Solid NaOMe (83 mg, 1.54 mmol) was added to **4c** (444 mg, 0.61 mmol) in warm THF (20 mL). After 10 min stirring, a solution of Fe(NO₃)₃ × 9H₂O (248 mg, 0.61 mmol) in EtOH (7 mL) was added dropwise. The dark purple suspension was stirred for 30 min at RT and filtered over a bed of silica. The product was eluted with EtOH/THF 2:1 (50 mL) and dried under reduced pressure. The residue was taken into CHCl₃ (5 mL) and purified on a short pad of Al₂O₃ by consecutive elution with CHCl₃ (100 mL), THF (100 mL), and finally EtOH (120 mL). After evaporation of the EtOH fraction, the product was redissolved in CHCl₃ (10 mL) and centrifuged. The supernatant was evaporated under reduced pressure to give a purple waxy solid (266 mg, 52%). M.p. 227 °C (decomp.). IR (CHCl₃): 1604 cm⁻¹ (C=N). UV-vis (CH₂Cl₂): λ_{max} (ε) = 497 nm (4760 M⁻¹cm⁻¹). HR-MS (ESI, MeOH): Calcd. for C₄₄H₇₂FeN₄O₄ [M – NO₃]⁺ $m/z = 776.4903$, found $m/z = 776.4885$. Anal. found (calcd) for C₄₄H₇₂N₅O₇Fe (838.93): C 63.10 (62.99), H 8.73 (8.65), N 8.36 (8.35).

Synthesis of 7e. Triethylenetetramine (175 mg, 1.2 mmol) was dissolved in EtOH (6 mL) and treated with a solution of **3e** (1.17 g, 2.4 mmol) in THF (18 mL). After 10 min, solid NaOMe (178 mg, 3.3 mmol) was added and the yellowish suspension was stirred for 10 min. An ethanolic solution of Fe(NO₃)₃ × 9H₂O (481 mg, 1.2 mmol in 9 mL) was then added dropwise. The dark purple suspension was stirred at RT for 30 min and filtered over a bed of silica. The product was eluted with EtOH/THF 2:1 (90 mL) and evaporated at reduced pressure. The residue was dissolved in CHCl₃ and purified on a short pad of Al₂O₃ (5 cm) using as eluents first CHCl₃ (70 mL) and subsequently EtOH/THF 2:1 (250 mL). Evaporation of the EtOH/THF fraction, the product was redissolved in CHCl₃ (20 mL) and centrifuged. The supernatant was evaporated at reduced pressure to give **7e** as a dark purple wax (1.30 g, 48%). Analytically pure material was obtained from a hexane (120 mL) solution upon extraction with MeOH (3 × 15 mL). M.p. 191 °C (decomp.). IR (CHCl₃): 1602 cm⁻¹ (C=N). UV-vis (CH₂Cl₂): λ_{max} (ε) = 496 nm (4180 M⁻¹cm⁻¹). HR-MS (ESI): calcd for C₆₆H₁₀₀FeN₄O₈ [M – NO₃]⁺ $m/z = 1132.6885$, found $m/z = 1132.6885$. Anal. found (calcd) for C₆₆H₁₀₀FeN₅O₁₁ (1195.4) × MeOH: C 65.13 (65.56); H 8.13 (8.54); N 5.40 (5.71).

Synthesis of 7f. According to procedure **7e**, reaction of triethylenetetramine (57 mg, 0.39 mmol) in EtOH (2 mL), **3f** (463 mg, 0.78 mmol) in THF (6 mL), NaOMe (58 mg, 1.07 mmol) with ethanolic Fe(NO₃)₃ × 9H₂O (157 mg, 0.39 mmol in 3 mL) gave **7f** as a dark purple wax (289 mg, 52%). Analytically pure complex was obtained from a hexane (120

mL) solution by extraction with MeOH (2 × 25 mL). M.p. 181 °C (decomp.). IR (CHCl₃): 1603 cm⁻¹ (C=N). UV-vis (CH₂Cl₂): λ_{max} (ε) = 497 nm (3460 M⁻¹cm⁻¹). HR-MS (ESI): calcd for C₈₂H₁₃₂FeN₄O₈ [M - NO₃]⁺ m/z = 1356.9389, found m/z = 1356.94025. Anal. found (calcd) for C₈₂H₁₃₂N₅O₁₁Fe (1419.83): C 69.47 (69.37); H 9.35 (9.37); N 4.82 (4.93).

Synthesis of 7g. According to procedure 7e, the reaction of triethylenetetramine (80 mg, 0.55 mmol) in EtOH (3 mL), 3g (842 mg, 1.10 mmol) in THF (8 mL), NaOMe (58 mg, 1.07 mmol) with ethanolic Fe(NO₃)₃ × 9H₂O (222 mg, 0.55 mmol) in 4 mL gave 7g as a dark purple wax (317 mg, 33%). An analytically pure sample was obtained by extraction of a hexane solution (120 mL) of 7g with MeOH (3 × 30 mL). M.p. 188 °C (decomp.). IR (CHCl₃): 1602 cm⁻¹ (C=N). UV-vis (CH₂Cl₂): λ_{max} (ε) = 496 nm (3900 M⁻¹cm⁻¹). HR-MS (ESI, MeOH): calcd for C₁₀₆H₁₈₀FeN₄O₈ [M - NO₃]⁺ m/z = 1693.3145, found m/z = 1693.3148. Anal. found (calcd) for C₁₀₆H₁₈₀N₅O₁₁Fe (1756.47) × MeOH: C 71.81 (71.86); H 10.33 (10.37); N 3.70 (3.92).

Langmuir Measurements

Pressure-area isotherms and time stability were measured at 25 °C on a KSV MiniMicro Langmuir-Blodgett trough (KSV, Finland) with a surface area between 1700 and 8700 mm². Water was purified with a Barnstead Nanopure system (Thermo Scientific), and its resistivity was measured to be higher than 18 MΩ cm. Chloroform (puriss. p.a. ≥ 99.8%, Fluka) was used as spreading solvent. Typically drops of the surfactant solution (20 μL, 0.50 mM) were deposited using a microsyringe on the water subphase. After letting the solvent evaporate for 30 min, the barriers were compressed at 6 mm min⁻¹ (3 cm² min⁻¹) and the surface pressure was monitored using a platinum Willhelmy plate.

Acknowledgments

We thank Prof. H. Möhwald for valuable discussions. This work was financially supported by ERA-net Chemistry. M.A. is very grateful for an Alfred Werner Assistant Professorship.

Notes and references

^a Department of Chemistry, University of Fribourg, Chemin du Musée 9, CH-1700 Fribourg, Switzerland.

^b Max Planck Institute of Colloids and Interfaces, D-14424 Potsdam, Germany; present address: Chemische Technologie der Materialsynthese, Universität Würzburg, Am Röntgenring 11, 97070 Würzburg, Germany

^c School of Chemistry and Chemical Biology, University College Dublin Belfield, Dublin 4, Ireland. Fax: +353 17162501; Tel: +353 17162504;

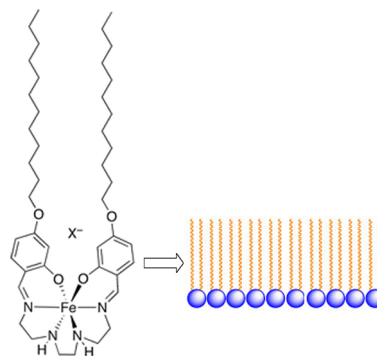
^d E-mail: martin.albrecht@ucd.ie

† Synthetic procedures for the synthesis of the ligands, pressure-area isotherms of complexes 6, stability plots of films comprising the cobalt(III) complexes and the iron(III) complexes 7e-g, and Brewster angle microscopy images for 7d. See DOI: 10.1039/b000000x/

- (a) E. Breuning, M. Ruben, J. M. Lehn, F. Renz, Y. Garcia, V. Ksenofontov and P. Gütllich, *Angew. Chem. Int. Ed.*, 2000, **39**, 2504. (b) M. Ruben, J. Rojo, F. J. Romero-Salguero, L. H. Uppadine and J.-M. Lehn, *Angew. Chem. Int. Ed.*, 2004, **43**, 3644. (c) M. L. Tang, A. D. Reichardt, N. Miyaki, R. M. Stoltenberg and Z. Bao, *J. Am. Chem. Soc.*, 2008, **130**, 6064.
- (a) O. Kahn, *Molecular Magnetism* (VCH), New York, 1993. (b) P. Gütllich, Y. Garcia and H. Spiering, in *Magnetism: Molecules to*

- Materials IV*; J. S. Miller, M. Drillon, eds. Wiley-VCH, Weinheim, Germany, 2002, p 271. (c) P. Gütllich, A. Hauser and H. Spiering, *Angew. Chem. Int. Ed. Engl.*, 1994, **33**, 2024. (d) J. A. Real, A. B. Gaspar, V. Niel and M. C. Munoz, *Coord. Chem. Rev.*, 2003, **236**, 121. (e) O. Sato, *Acc. Chem. Res.*, 2003, **36**, 692. (f) P. Gütllich and H. A. Goodwin, *Top. Curr. Chem.*, 2004, **233**, 1. (g) J.-F. Letard, P. Guionneau and L. Goux-Capes, *Top. Curr. Chem.*, 2004, **235**, 221. For key examples relevant to this work, see: (h) J. A. Real, E. Andres, M. C. Munoz, M. Julve, T. Granier, A. Bousseksou and F. Varret, *Science*, 1995, **268**, 265. (i) O. Kahn and C. J. Martinez, *Science*, 1998, **279**, 44. (j) S. Hayami, Z. Gu, H. Yoshiki, A. Fujishima and O. Sato, *J. Am. Chem. Soc.*, 2001, **123**, 11644. (k) M. Seredyuk, A. B. Gaspar, V. Ksenofontov, Y. Galyametdinov, J. Kusz and P. Gütllich, *J. Am. Chem. Soc.*, 2008, **130**, 1431. (l) S. Cobo, D. Ostrovskii, S. Bonhommeau, L. Vendier, G. Molnar, L. Salmon, K. Tanaka and A. Bousseksou, *J. Am. Chem. Soc.*, 2008, **130**, 9019. (m) S. Brooker and J. A. Kitchen, *Dalton Trans.*, 2009, 7331.
- Similarly, redox activity may be engineered to obtain conducting and semiconducting materials: (a) C. Joachim, J. K. Gimzewski and A. Aviram, *Nature*, 2000, **408**, 541. (b) Z. Bao, *Adv. Mater.*, 2000, **12**, 227. (c) R. Naaman and Z. Vager, *Acc. Chem. Res.*, 2003, **36**, 291. (d) A. Schenning and E. W. Meijer, *Chem. Commun.*, 2005, 3245. for recent examples, see: (e) M. Lemieux, M. Roberts, S. Y. W. Barman, Jin, J. M. Kim and Z. Bao, *Science*, 2008, **321**, 101.
- (a) J.-M. Lehn, *Supramolecular Chemistry* (Wiley-VCH), Weinheim, 1995. (b) J. M. Lehn, *Science*, 2002, **295**, 2400. (c) J. C. Love, L. A. Estroff, J. K. Kriebel, R. G. Nuzzo and G. M. Whitesides, *Chem. Rev.*, 2005, **105**, 1103.
- (a) M. Ruben, U. Ziener, J.-M. Lehn, V. Ksenofontov, P. Gütllich and G. B. M. Vaughan, *Chem. Eur. J.*, 2005, **11**, 94. (b) Y. Bodenthin, U. Pietsch, H. Möhwald and D. G. Kurth, *J. Am. Chem. Soc.*, 2005, **127**, 3110. (c) S. Cobo, G. Molnar, J. A. Real and A. Bousseksou, *Angew. Chem. Int. Ed.*, 2006, **45**, 5786. (d) A. B. Gaspar, M. Seredyuk and P. Gütllich, *Coord. Chem. Rev.*, 2009, **253**, 2399. (e) Y. Bodenthin, G. Schwarz, Z. Tomkowicz, M. Lommel, T. Geue, W. Haase, H. Möhwald, U. Pietsch and D. G. Kurth, *Coord. Chem. Rev.*, 2009, **253**, 2414.
- For an example from catalysis: M. Albrecht, N. J. Hovestad, J. Boursma and G. van Koten, *Chem. Eur. J.*, 2001, **7**, 1289.
- (a) G. Decher, *Science*, 1997, **277**, 1232. (b) N. Miyashita and D. G. Kurth, *J. Mater. Chem.*, 2008, **18**, 2636.
- (a) J. F. Quinn, A. P. R. Johnston, G. K. Such, A. N. Zelikin and F. Caruso, *Chem. Soc. Rev.*, 2007, **36**, 707. (b) S. Srivastava and N. A. Kotov, *Acc. Chem. Res.*, 2008, **41**, 1831. (c) Q. He, Y. Cui and J. Li, *Chem. Soc. Rev.*, 2009, **38**, 2292.
- (a) M. F. Tweedle and L. J. Wilson, *J. Am. Chem. Soc.*, 1976, **98**, 4824. (b) E. Sinn, G. Sim, E. V. Dose, M. F. Tweedle and L. J. Wilson, *J. Am. Chem. Soc.*, 1978, **100**, 3375. (c) R. Pritchard, S. A. Barrett, C. A. Kilner and M. A. Halcrow, *Dalton Trans.*, 2008, 3159.
- P. N. Martinho, C. J. Harding, H. Müller-Bunz, M. Albrecht and G. G. Morgan, *Eur. J. Inorg. Chem.*, in press.
- (a) K. B. Blodgett, *J. Am. Chem. Soc.*, 1934, **56**, 495. (b) K. B. Blodgett and I. Langmuir, *Phys. Rev.*, 1937, **51**, 964. (c) D. R. Talham, *Chem. Rev.*, 2004, **104**, 5479.
- (a) M. D. Hollingsworth, *Science*, 2002, **295**, 2410. (b) M. Hostettler, K. W. Törnroos, D. Chernyshov, B. Vangdal and H.-B. Bürgi, *Angew. Chem. Int. Ed.*, 2004, **43**, 4589. (c) C. Felser, G. H. Fecher and B. Balke, *Angew. Chem. Int. Ed.*, 2007, **46**, 668.
- (a) C. Mingotaud, P. Delhaes, M. W. Meisel and D. R. Talham, in *Magnetism: Molecules to Materials II: Molecule-Based Materials*; J. S. Miller, M. Drillon, eds. Wiley-VCH, Weinheim, Germany, 2002, p. 457. (b) P. Coronel, A. Barraud, R. Cluade, O. Kahn, A. Ruauadel-Teixier and J. Zarembowitch, *J. Chem. Soc., Chem. Commun.*, 1989, 193. (c) D. G. Kurth, P. Lehmann and M. Schütte, *Proc. Nat. Acad. Sci.*, 2000, **97**, 5704. (d) O. Roubeau, B. Agricole, R. Clerac and S. Ravaine, *J. Phys. Chem. B.*, 2004, **108**, 15110.
- (a) H. Soyer, C. Mingotaud, M.-L. Boillot and P. Delhaes, *Langmuir*, 1998, **14**, 5890. (b) H. Soyer, E. Dupart, C. J. Gomez-Garcia, C. Mingotaud and P. Delhaes, *Adv. Mater.*, 1999, **11**, 382.
- C. Gandolfi, C. Moitzi, P. Schurtenberger, G. G. Morgan and M. Albrecht, *J. Am. Chem. Soc.*, 2008, **130**, 14434.
- P. Zell, F. Mögele, U. Ziener and B. Rieger, *Chem. Eur. J.*, 2006, **12**, 3847.

- 17 C. J. Hawker and J. M. J. Frechet, *J. Am. Chem. Soc.*, 1990, **112**, 7638.
- 18 (a) B. D. Sarma and J. C. Bailar, *J. Am. Chem. Soc.*, 1955, **77**, 5476.
 (b) Y. Yamamoto and S. Tsukuda, *Bull. Chem. Soc. Jpn.*, 1985, **58**, 1509. (c) A. S. Rothin, H. J. Banbery, F. J. Berry, T. A. Hamor, C. J. Jones and J. A. McCleverty, *Polyhedron*, 1989, **8**, 491.
- 19 See the supporting material for further details.
- 20 K. M. Kadish, K. Das, D. Schaeper, C. L. Merrill, B. R. Welch and L. J. Wilson, *Inorg. Chem.*, 1980, **19**, 2816.
- 21 M. Krejciak, M. Danek and F. Hartl, *J. Electroanal. Chem.*, 1991, **317**, 179.
- 22 Attempts to reduce complexes **7** chemically by using an excess of CrCl₂ induced the substitution of the hexadentate coordinated metal center from Fe³⁺ to Cr³⁺ only, as indicated by the pertinent mass spectrometric data.
- 23 (a) B. Lin, M. C. Shih, T. M. Bohanon, G. E. Ice and P. Dutta, *Phys. Rev. Lett.*, 1990, **65**, 191. (b) S. Ramos and R. Castillo, *J. Chem. Phys.*, 1999, **110**, 7021. (c) R. Johann and D. Vollhardt, *Mater. Sci. Eng., C*, 1999, **8–9**, 35. (d) R. Johann, D. Vollhardt and H. Möhwald, *Langmuir*, 2001, **17**, 4569.
- 24 D. K. Chattoraj, E. Halder, K. P. Das and A. Mitra, *Adv. Colloid Interface Sci.*, 2006, **123–126**, 151.
- 25 T. Hasegawa, Y. Iiduka, H. Kakuda and T. Okada, *Anal. Chem.*, 2006, **78**, 6121.
- 26 M. C. Petty, *Langmuir-Blodgett Film: An Introduction*; Cambridge University Press: Cambridge, 1996.
- 27 R. Popovitz-Biro, K. Hill, E. M. Landau, M. Lahav, L. Leiserowitz, J. Sagiv, H. Hsiung, G. R. Meredith and H. Vanherzeele, *J. Am. Chem. Soc.*, 1988, **110**, 2672.
- 28 (a) K. Sivanandan, S. V. Aathimanikandan, C. G. Arges, C. J. Bardeen and S. Thayumanavan, *J. Am. Chem. Soc.*, 2005, **127**, 2020. (b) Z. Bo, X. Zhang, X. Yi, M. Yang, J. Shen, Y. Ren and S. Xi, *Polym. Bull.*, 1997, **38**, 257. (c) Y. Azeffu, H. Tamiaki, R. Sato and K. Toma, *Bioorg. & Med. Chem.*, 2002, **10**, 4013.
- 29 (a) S. Inoue, T. Yanai, S. Ando, A. Nakazawa, K. Honda, Y. Hoshino and T. Asai, *J. Mater. Chem.*, 2005, **15**, 4746. (b) I. Aiello, M. Ghedini, M. La Deda, D. Pucci and O. Francescangeli, *Eur. J. Inorg. Chem.*, 1999, 1367.
- 30 N. G. Connelly and W. E. Geiger, *Chem. Rev.*, 1996, **96**, 877.



For table of contents use

Organization of spin- and redox-labile metal centers into Langmuir and Langmuir-Blodgett films

*C. Gandolfi, N. Miyashita, D. G. Kurth, P. N. Martinho, G. G. Morgan, M. Albrecht**

- Electronically and magnetically switchable iron and cobalt complexes comprising an amphiphilic alkoxy-functionalized sal₂(trien) ligand self-assemble at the air-water interface, forming stable Langmuir films provided the alkoxy-tails are sufficiently long. Transfer of the films to a support affords unusual Z-type layers.